arXiv:cond-mat/0309365v1 [cond-mat.stat-mech] 16 Sep 2003

Kinetic Roughening of Ion-Sputtered Pd(001) Surface: Beyond the Kuramoto-Sivashinsky Model

T. C. Kim,[1] C.-M. Ghim,[2,*] H. J. Kim,[1] D. H. Kim,[1] D. Y. Noh,[1] N. D. Kim,[3]
J. W. Chung,[3] J. S. Yang,[4] Y. J. Chang,[4] T. W. Noh,[4] B. Kahng,[2] and J.-S. Kim[5,†]

[1]*Department of Materials Science and Engineering, Kwangju Institute of Science and Technology, Gwangju, 500-712, Korea*
[2]*School of Physics and Center for Theoretical Physics, Seoul National University, Seoul 151-747, Korea*
[3]*Department of Physics and Basic Science Research Institute, Pohang University of Science and Technology, Pohang 790-784, Korea*
[4]*School of Physics and Research Center for Oxide Electronics, Seoul National University, Seoul 151-747, Korea*
[5]*Department of Physics, Sook-Myung Women's University, Seoul 140-742, Korea*

(Dated: February 2, 2008)

We investigate the kinetic roughening of Ar^+ ion-sputtered Pd(001) surface both experimentally and theoretically. *In situ* real-time x-ray reflectivity and *in situ* scanning tunneling microscopy show that nanoscale adatom islands form and grow with increasing sputter time t. Surface roughness, $W(t)$, and lateral correlation length, $\xi(t)$, follows the scaling laws, $W(t) \sim t^{\beta}$ and $\xi(t) \sim t^{1/z}$ with the exponents $\beta \simeq 0.20$ and $1/z \simeq 0.20$, for ion beam energy $\varepsilon = 0.5$ keV, which is inconsistent with the prediction of the Kuramoto-Sivashinsky (KS) model. We thereby extend the KS model by applying the Sigmund theory of sputter erosion to the higher order, $O(\nabla^4, h^2)$, where h is surface height, and derive a new term of the form $\nabla^2(\nabla h)^2$ which plays an indispensable role in describing the observed morphological evolution of the sputtered surface.

PACS numbers: 68.55.-a, 05.45.-a, 64.60.Cn, 79.20.Rf

Recently, the observation of ordered nanostructures such as ripples and two-dimensional patterns on ion-sputtered surfaces has attracted much attention due to the demonstration of the possibility of fabrication of ordered nanoscale structures in a relatively easy and affordable way [1, 2, 3, 4, 5, 6, 7]. Such experimental results have motivated extensive theoretical investigations aiming to understand the mechanism of the morphological evolution of ion-sputtered surfaces. A linear model, proposed by Bradley and Harper (BH) [8], has been successful in predicting the formation of the ripple structure. The wavelength, orientation and amplitude of the ripples can be predicted in terms of experimental parameters such as the incident angle of the ion beam and substrate temperature [9]. The BH theory, however, fails to explain a number of experimental observations such as the saturation of the ripple amplitude [10, 11, 12], or the appearance of kinetic roughening [13, 14]. To remedy such shortcomings, the noisy Kuramoto-Sivashinsky (KS) equation [15, 16] was introduced based on the Sigmund theory of sputter erosion [17]. In addition to the linear terms of the BH model, it contains a nonlinear term proportional to $(\nabla h)^2$, known as the Kardar-Parisi-Zhang (KPZ) term [18], where h is surface height. Due to the nonlinear term, the surface roughness (or the ripple amplitude), which was growing exponentially with increasing sputter time in the linear model, changes to the type following a power law and eventually saturates to a constant value [19]. Although the KS model seems to be successful in offering insights for understanding the nonlinear behavior of sputter-eroded surfaces, it has not been convincing yet because the detailed properties of the kinetic roughening predicted by the KS equation have not been fully tested experimentally.

Kinetic roughening behavior is described by the scaling theory [20]. The surface roughness of the sample, $L \times L$ in size, at sputter time t is defined as $W \equiv \sqrt{(1/L^2)\sum_{\mathbf{r}} \left[h(\mathbf{r},t) - \bar{h}\right]^2}$, where $\bar{h} = (1/L^2)\sum_{\mathbf{r}} h(\mathbf{r},t)$. It follows the scaling relation, $W(L,t) \sim L^{\alpha} g(t/L^{\alpha/\beta})$, where $g(u) \sim u^{\beta}$ for $u \ll 1$ and $g(u \to \infty) \sim$ constant. The roughness and growth exponents α and β are related via scaling relations to give the dynamic exponent, $z = \alpha/\beta$, which determines the scaling of the saturation time with the system size L. Below, we will deal with the inverse dynamic exponent, $1/z$, called the coarsening exponent, in analyzing the experimental results.

In this Letter, we study the kinetic roughening of sputter-eroded Pd(001) surface via novel experimental techniques combined with the stochastic continuum theory. Both *in situ* real-time X-ray reflectivity (XRR) and *in situ* scanning tunneling microscopy (STM) show that nanoscale islands are formed on surface, evolving with increasing sputter time t following the scaling function $W(L,t)$. In particular, we obtain $\beta \simeq 0.2$ and $1/z \simeq 0.2$ for ion beam energy $\varepsilon = 0.5$ keV, which are not in agreement with the values predicted by the KS model. To resolve this inconsistency, we investigate theoretically the erosion process by applying the Sigmund theory to higher order, finding that the relevant higher order term is of the form $\nabla^2(\nabla h)^2$, referred to as the conserved KPZ (cKPZ) term. Using this new nonlinear term, we can explain the kinetic roughening on the sputtered Pd(001) surface successfully.

Experiment.—A Pd(001) sample was cleaned by several cycles of Ar^+ ion sputtering around 300 K and annealing up to 920 K. The clean Pd(001) surface exhibited an average terrace size of about 3000 Å and little surface modulation or defects by contaminants as judged by STM images. The initial surface roughness of the sample was less than 2 Å and the miscut from surface normal direction was 0.3°, as determined

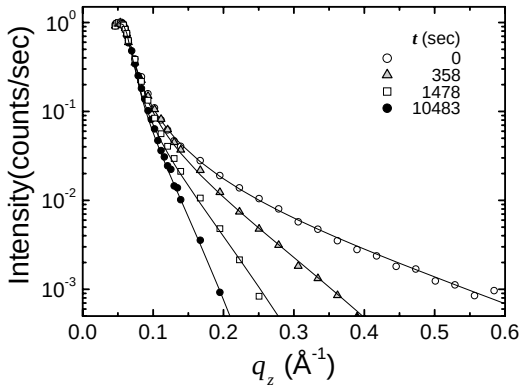

FIG. 1: Specular x-ray reflectivity (symbols) as a function of the momentum transfer, q_z, for increasing sputter times with $\varepsilon = 0.5$ keV and $f = 2.0 \times 10^{13}$ ions/cm^2/sec. Sputtering is made normal to a sample at room temperature. The solid lines are the theoretical ones according to the Parratt formula.

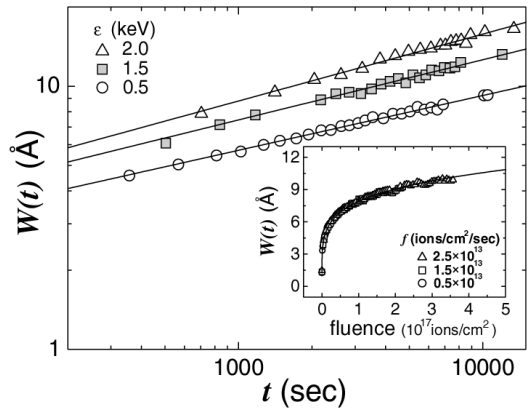

FIG. 2: The surface roughness W as a function of sputter time t for different ion energies, $\varepsilon = 0.5(\bigcirc)$, $1.5(\square)$, and $2.0(\triangle)$ keV, but with a fixed ionic flux, $f = 2.0 \times 10^{13}$ ions/cm^2/sec. Inset shows that the roughness evolution for a given ε follows the same fluence dependence, irrespective of f.

respectively by X-ray reflectivity (XRR) and X-ray diffraction spot-profile analysis. Sputtering experiments were performed for Pd(001) around 300 K with Ar^+ ion beam incident normally to the sample surface. To avoid possible contamination during sputtering, fresh Ar gas (purity of 99.999%) was continuously made to flow through the chamber with Ar partial pressure maintained around 2.0×10^{-5} Torr.

The morphological evolution of the Pd(001) during sputtering was observed *in situ* by both XRR and STM. The XRR experiment was performed in a custom-designed UHV chamber at the 5C2 K-JIST beamline of the Pohang Light Source in Korea. The base pressure of the chamber was kept below mid-10^{-10} Torr. The incident X-rays were vertically focused by a mirror to 1 mm in size, and a double-bounce Si(111) monochromator was employed to both focus the beam in the horizontal direction and monochromatize the incident X-ray to a wavelength of 1.24 Å which corresponded to the X-ray

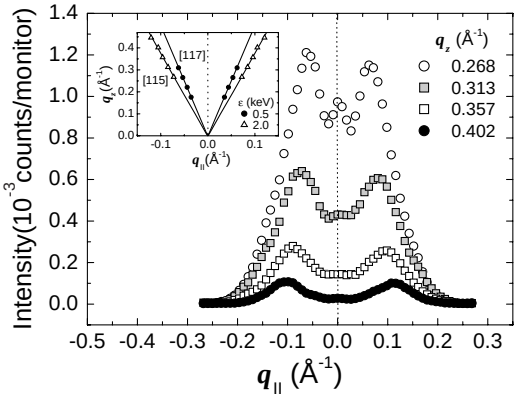

FIG. 3: X-ray diffraction intensity along [110] for different q_z. The positions of satellite peaks shift to the larger $q_{||}$ for the larger q_z, with a fixed angle to the surface normal, indicating that the spots originate from a facet formed by sputtering. Inset: Plot of the positions of satellite peaks, $q_{||}$, as a function of q_z. From the angle the facet peaks form with respect to the surface normal, we identify the facet planes to be (117) for $\varepsilon = 0.5$ keV and (115) for $\varepsilon = 2.0$ keV.

energy of 10 keV. The X-ray reflectivity was measured in real time while Pd(001) was sputtered. Incident Ar^+ beam energy, ε, ranged from 0.5 to 2.0 keV, and ion beam flux, f, measured from the ion current collected at the sample, ranged from 0.5×10^{13} to 2.5×10^{13} ions/cm^2/sec. Sputtering started with the sample at room temperature measured by a thermocouple directly attached to the back-end of the sample. After sputtering for more than 10 hours, the sample temperature rose only less than 30 K.

To observe the sputter-induced morphological evolution in real-space, a commercial STM (Omicron VT-STM) was also used. The base pressure was kept in the low 10^{-11} Torr. STM tips were electro-chemically etched polycrystalline W-wires that were annealed and sputtered in a UHV chamber. In all the STM measurements, the tip-sample voltage was kept as 80 mV, and the tunneling current was at 1 nA with the sample at room temperature. Sputtering was performed with $\varepsilon = 0.5$ keV and $f = 0.5 \times 10^{13}$ ions/cm^2/sec. During sputtering, the sample temperature was around 300 K. Sputtering and STM measurement were alternated, and the sputter time referred to in the present work is the total sputter time determined by summing all the previous sputtering periods. X-ray reflectivity indicated that there was no significant change in the surface roughness for 10 hours after the interruption of sputtering. Thus, the interruption of sputtering for the STM measurement was not expected to result in additional relaxation of the sputtered surface.

Experimental results.—In Born approximation which holds above critical angle, the specular reflectivity decreases as $\exp(-W^2 q_z^2)$ with increasing q_z [21]. Fig. 1 shows that the reflectivity decays more steeply as the sputtering proceeds, which indicates that $W(t)$ increases with t. Quantitatively $W(t)$ is determined by fitting the experimental data according to the Parratt formalism [21, 22]. Fig. 2 shows $W(t)$ thus

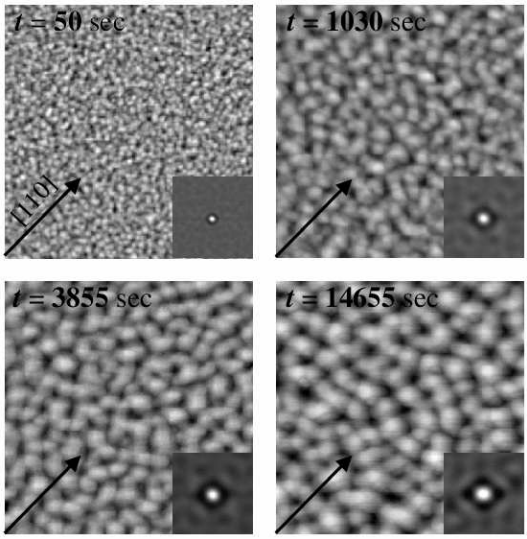

FIG. 4: STM images for various sputtering times which are 200 × 200 nm^2 in size. The insets at right bottom of each image show the height-height correlation function obtained from the corresponding surface profile.

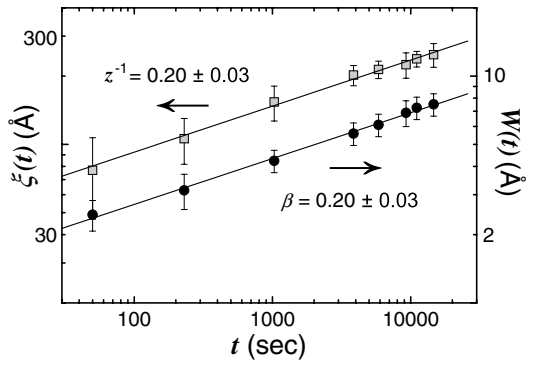

FIG. 5: Plot of the lateral correlation length $\xi(\bigcirc)$ and the surface roughness $W(\square)$ obtained from the STM images as a function of sputter time t.

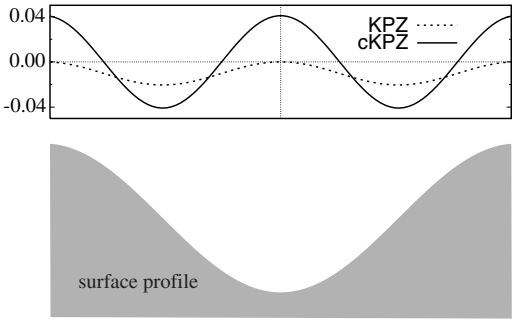

FIG. 6: Comparison of the KPZ and the cKPZ terms for a prototypical profile of eroded surface.

obtained, as a function of t for several ε but with a fixed f. The linear behavior in double-logarithmic scale implies power-law behavior, $W(t) \sim t^{\beta}$. We obtained that $\beta \simeq 0.20 \pm 0.02$ for $\varepsilon = 0.5$ keV, $\beta \simeq 0.23 \pm 0.02$ for $\varepsilon = 1.5$ keV, and $\beta \simeq 0.25 \pm 0.02$ for $\varepsilon = 2.0$ keV.

The inset of Fig. 2 summarizes the surface roughness, $W(t)$ as a function of fluence ($f \times t$) for several different fs, but with a fixed ε. We find that the roughness evolves showing the same fluence dependence, irrespective of f. Such behavior implies that the surface diffusion is not induced by thermal activation, but rather by the surface sputtering under the present experimental condition [23].

We also study the facet formation on the sputtered surface by tracing the extra-diffraction peaks or satellites around the diffraction peak corresponding to the sample surface, now (001) plane, because each facet plane defines diffraction rods normal to it. In the inset of Fig. 3, the diffraction rods defined by the satellite peaks make well-defined angles with respect to that of (001) plane as much as the facet plane does to the (001) plane . From the observed angles, we identify the facet formed on sputtering by 0.5 keV ion beam to be (117) and that by 2.0 keV beam to be (115).

The morphological evolution of the sputtered Pd(001) surface were also investigated by an STM. Fig. 4 shows the STM images of the sputtered surface at different (total) sputtering time under the same experimental condition, $\varepsilon = 0.5$ keV and $f = 0.5 \times 10^{13}$ ions/cm^2. The shape of the island edge looks somewhat irregular which may be due to random shot noise or the sputter-induced diffusion. This reaffirms that thermal smoothening is inefficient in the present experimental conditions as suggested by the flux-independent scaling behavior. The insets of Fig. 4 show the height-height correlation function, $G(r,t) = \langle (h(r,t) - h(0,0))^2 \rangle$, that reveals lateral order developing on the surface as sputtering proceeds. We can see that the island size grow with increasing sputter time. From the height-height correlation function, we determine the lateral correlation length, ξ, as the position giving the first-order maximum [24], and plot it as a function of t in Fig. 5. It is found that $\xi \sim t^{1/z}$ with the exponent $1/z \simeq 0.20 \pm 0.03$. The growth exponent determined by the STM measurement is $\beta \simeq 0.20 \pm 0.03$, in agreement with that of the XRR measurement.

Theory.—To elucidate the kinetic roughening, we systematically expand the Sigmund theory to higher order than that where the KS equation is derived, and obtain the dynamic equation,

$$\frac{1}{c}\frac{\partial h}{\partial t} = -1 - \nu\nabla^2 h - D\nabla^4 h + \lambda_1(\nabla h)^2 + \lambda_2\nabla^2(\nabla h)^2 + \eta(x,y,t)\,, \tag{1}$$

where c is the surface recession rate given by the material constant times the ionic flux, ν the effective surface tension generated by the erosion process, D the ion-induced effective diffusion constant [23], λ_1 and λ_2 the tilt-dependent erosion rate, and η an uncorrelated white noise with zero mean, mimicking the randomness resulting from the stochastic nature of ion arrival at the surface. The coefficients ν, D, and λ_1 in

Eq. (1) were derived in terms of experimental parameters such as the ion beam energy ε, the flux f, the incident angle θ, the penetration depth a, and the cascading sizes in transverse and longitudinal directions, μ and σ respectively [16]. The newly derived cKPZ coefficient is, under normal incidence, given by $\lambda_2 = \mu^2/2 + (3/8)(\mu/\sigma)^4(\sigma^2 - a^2)$. Using the TRIM Monte Carlo algorithm [25], all the coefficients in Eq. (1) are determined numerically for our experimental parameters, which are tabulated in Table I. In Fig. 6, is shown the estimation of the KPZ and cKPZ terms, for a typical profile of the eroded surface. We find that the cKPZ term should be more relevant to the morphological evolution than the KPZ term in a finite system. The contributions from other terms allowed by symmetry and of order $o(\nabla^4, h^2)$ such as $(\nabla^2 h)^2$, are found to be negligible. Then, for $\varepsilon = 0.5$ keV, the extended KS equation is reduced to the cKPZ equation that gives the growth exponent $\beta \simeq 0.20$ [26] for two dimensions, in agreement with the measured value for $\varepsilon = 0.5$ keV. As the ion energy increases, the coefficient D increases very rapidly in comparison with the magnitudes of the λ_1 and λ_2 as seen in the Table I. Thus, for the $\varepsilon = 2.0$ keV, the erosion process is mainly governed by the so-called Mullins term, $D\nabla^4 h$ [27]. In this case, it is known that the growth exponent $\beta \simeq 0.25$ for two dimensions, again consistent with the experimental value for $\varepsilon = 2.0$ keV. The sputter-induced palladium atoms form adatom islands with well-defined facets as observed in Fig. 3. Then, $\alpha = 1$ and the coarsening exponent, $1/z$, should be equal to β following the scaling relation $1/z = \beta/\alpha$. This prediction is confirmed in the present experiment, by the observation of $1/z = \beta = 0.2$ for $\varepsilon = 0.5$ keV.

ε	ν	D	λ_1	λ_2
0.5 keV	2.72	33.35	-0.50	12.2
1.5 keV	5.12	184.32	-0.54	33.6
2.0 keV	5.44	266.78	-0.50	49.0

TABLE I: Numerical estimations of the coefficients in Eq.(1) under the experimental conditions we performed.

Conclusions.—We have studied the kinetic roughening of the sputter-eroded Pd(001) surface both experimentally and theoretically. The experimental data suggest that the KS continuum model is not relevant to the morphological evolution of the Pd surface. Instead, the KS model extended by the inclusion of the cKPZ term we derived from the Sigmund theory could properly describe the kinetic roughening behavior of the sputtered Pd(001) surface. The model, at the same time, may shed light on recent experimental realization of self-organized surface nanostructures induced by ion sputtering. For example, the parameter space for nanoscale island formation predicted by the KS model, which seems too narrow to be realistic as compared with experimental observations [28], can be enhanced.

This work is supported by the Korean Research Foundation (KRF-2002-015-CP0087) through SMU and KOSEF Grant No.2002-2-11200-002-3 in the BRP program through SNU.

* Electronic address: cmghim@phya.snu.ac.kr
† Electronic address: jskim@sookmyung.ac.kr

[1] S. Facsco, T. Dekorsy, C. Koerdt, C. Trappe, H. Kurz, A. Vogt, H. L. Hartnagel, Science **285**, 1551 (1999).
[2] F. Frost, A. Schindler, and F. Bigl, Phys. Rev. Lett. **85**, 4116 (2000).
[3] S. Rusponi, C. Boragno, and U. Valbusa, Phys. Rev. Lett. **78**, 2795 (1997); S. Rusponi, G. Costantini, C. Boragno, and U. Valbusa, Phys. Rev. Lett, **81**, 2735 (1998); *ibid*, **81**, 4184 (1998).
[4] J. C. Girard, Y. Samson, S. Gautier, S. Rousset, and J. Klein, Surf. Sci. **302**, 73 (1994).
[5] J. Naumann, J. Osing, A. J. Quinn, and I. V. Shvets, Surf. Sci. **388**, 212 (1997).
[6] E. Chason, T. M. Mayer, and B. K. Kellerman, Mat. Res. Soc. Symp. Proc., **396**, 143 (1996).
[7] *Sputtering by Particle Bombardment*, R. Behrisch, ed. (Springer-Verlag, Heidelberg, 1981, 1983) Vols. I, II.
[8] R. M. Bradley and J. M. E. Harper, J. Vac. Sci. Technol. A **6**, 2390 (1988).
[9] I. Koponen, M. Hautala. and O.-P. Sievanen, Phys. Rev. Lett. **78**, 2612 (1997).
[10] K. Wittmaack, J. Vac. Sci. Technol. A **8**, 2246 (1990).
[11] J. Erlebacher, M. J. Aziz, E. Chason, M. B. Sinclair, and J. A. Floro, preprint.
[12] J. J. Vajo, R. E. Doty, and E.-H. Cirlin, J. Vac. Sci. Technol. A **6**, 76 (1988).
[13] E. A. Eklund *et al*., Phys. Rev. Lett. **67**, 1759 (1991).
[14] H.-N. Yang, G.-C. Wang, and T.-M. Lu, Phys. Rev. B **50**, 7635 (1994).
[15] M. A. Makeev, R. Cuerno and A.-L. Barabási, cond-mat/0007354 (2000); Y. Kuramoto, *Chemical Oscillations, Waves and Turbulence* (Springer, Berlin, 1984).
[16] R. Cuerno and A. L. Barabási, Phys. Rev. Lett. **74**, 4746 (1995).
[17] P. Sigmund, Phys. Rev. **184**, 383 (1969).
[18] M. Kardar, G. Parisi, and Y.-C. Zhang, Phys. Rev. Lett. **56**, 889 (1986).
[19] S. Park, B. Kahng, H. Jeong, and A.-L. Barabási, Phys. Rev. Lett. **83**, 3486 (1999).
[20] A.-L. Barabási and H. E. Stanley, *Fractal Concepts in Surface Growth*, (Cambridge University Press, Cambridge, 1995).
[21] S. K. Sinha, E. B. Sirota, S. Garoff, and H. B. Stanley, Phys. Rev. B **38**, 2297 (1998).
[22] L. G. Parratt, Phys. Rev. **95**,359 (1954).
[23] M. A. Makeev and A.-L. Barabási, Appl. Phys. Lett. **71**, 2800 (1997).
[24] G. Constantini, S. Rusponi, R. Gianotti, C. Boragno, and U. Valbusa, Surf. Sci. **416**, 245 (1998).
[25] J. F. Ziegler, J. P. Biersack, and U. Littmark, *The Stopping and Range of Ions in Solids* (Pergamon Press, NY, 1996).
[26] Z.-W. Lai and S. Das Sarma, Phys. Rev. Lett. **66**, 2348 (1991); S. H. Yook, J. M. Kim, and Y. Kim, Phys. Rev. E **56**, 4085 (1997); Y. Kim, D. K. Park, J. M. Kim, J. Phys. A **27**, L533 (1994).
[27] W. W. Mullins, J. Appl. Phys. **28**, 333 (1957).
[28] B. Kahng, H. Jeong and A.-L. Barabási, Appl. Phys. Lett. **78**, 6 (2001).